Available online at www.sciencedirect.com
ScienceDirect
Bioorganic & Medicinal Chemistry 16 (2008) 1084–1089
Bioorganic & Medicinal Chemistry

Electronic effects of *para*-substitution on acetophenones in the reaction of rat liver 3α-hydroxysteroid dehydrogenase

Koji Uwai,* Noboru Konno, Yuka Yasuta and Mitsuhiro Takeshita*

Department of Pharmaceutics, Tohoku Pharmaceutical University, 4-4-1 Komatsushima, Aoba-ku, Sendai 981-8558, Japan

Received 6 October 2007; revised 29 October 2007; accepted 29 October 2007
Available online 4 November 2007

Abstract—Stereoselective reductive metabolism of various *p*-substituted acetophenone derivatives was studied using isolated rat liver 3α-hydroxysteroid dehydrogenase (3α-HSD). Kinetic experiments were performed and analyzed by measuring the products by HPLC using a chiral column. The results demonstrated that the presence of an electron-withdrawing substituent on the benzene ring plays an important role in determining the reduction rate in the syntheses of various (*S*)-alcohols from their corresponding carbonyl compounds. A plot of log $\{(V_{max}/K_m)X/(V_{max}/K_m)H\}$ versus the substituent parameter (π, σ_{para}, Es) shows an increasing rate mainly for electron-withdrawing substituents, with a correlation coefficient (r^2) of 0.97 which was obtained for triplicate data that were significant at the $p < 0.0001$ level. With this in mind, new drugs can be designed that exploit this reduction pathway by introducing an electron-withdrawing group adjacent to the reduction site when a reduction reaction is desired, or by adding an electron-donating group when minimization of the reduction pathway is desired.

1. Introduction

Enzymatic asymmetric reduction with an in situ NADPH-cofactor regeneration system using a 3α-hydroxysteroid dehydrogenase (3α-HSD) from rat liver (*Rattus norvegicus*) is very important for producing optically active alcohols and understanding the physiological phenomena of the dehydrogenase.

Rat liver 3α-HSD is involved in steroid hormone metabolism,[1] biosynthesis of bile acids,[2] detoxification of carcinogenic polycyclic aromatic hydrocarbons,[3] regulation of inflammatory prostaglandin levels,[4] detoxification of xenobiotic carbonyl compounds[1,5] and the metabolism of narcotic drugs as a drug-metabolizing enzyme.[6] This enzyme also plays an important role in the intracellular transport of bile acids from the sinusoidal to the canalicular pole of hepatocytes as a bile acid binder.[7] Despite its broad substrate specificity for carbonyl compounds, ketone-containing drugs such as daunorubicin, ketamine, warfarin and metyrapone were not reduced by the present enzyme. Thus, systematic studies of the relationships between structure and reducibility need to be performed.

In the course of our studies, we found that 2-, 3- and 4-acetyl pyridine derivatives were reduced by rat liver 3α-HSD at various rates.[8] Therefore, we assumed that the reduction rate was affected by the electron density of the carbonyl group. Thus, in this study, we report the substituent effects on the mechanism of reduction of acetophenone derivatives that were contained in the number of the structure of the drug, using rat liver 3α-HSD (Scheme 1).

2. Results and discussion

We employed nitro, cyano, bromo, methyl, methoxyl and dimethylamino groups as substituents at the *para*-

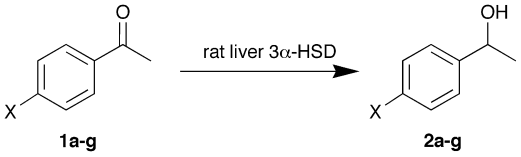

Scheme 1. Reduction of acetophenone derivatives by rat liver 3α-HSD. X = H (a); NO_2 (b); CN (c); Br (d); Me (e); OMe (f); NMe_2 (g).

Keywords: 3α-HSD; Metabolic enantioselective reduction; Hammett's reaction constant.
* Corresponding authors. Tel./fax: +81 22 727 0111; e-mail: uwai@tohoku-pharm.ac.jp

0968-0896/$ - see front matter © 2007 Elsevier Ltd. All rights reserved.
doi:10.1016/j.bmc.2007.10.096

position of acetophenone. All of the acetophenone derivatives were reduced enantioselectively by rat liver 3α-HSD to give (*S*)-alcohols. The stereochemistry of the formed alcohol was determined by comparison of the HPLC retention time of the product with synthesized authentic samples. The reaction rates were followed by Michaelis–Menten plots (Fig. 1), and the steady-state kinetic parameters of reduction of acetophenone derivatives **1a**–**g** were measured and are summarized in Table 1.

The kinetic parameters depend on the type of the substituent. The data show that the introduction of an electron-withdrawing group such as a nitro (**1b**),

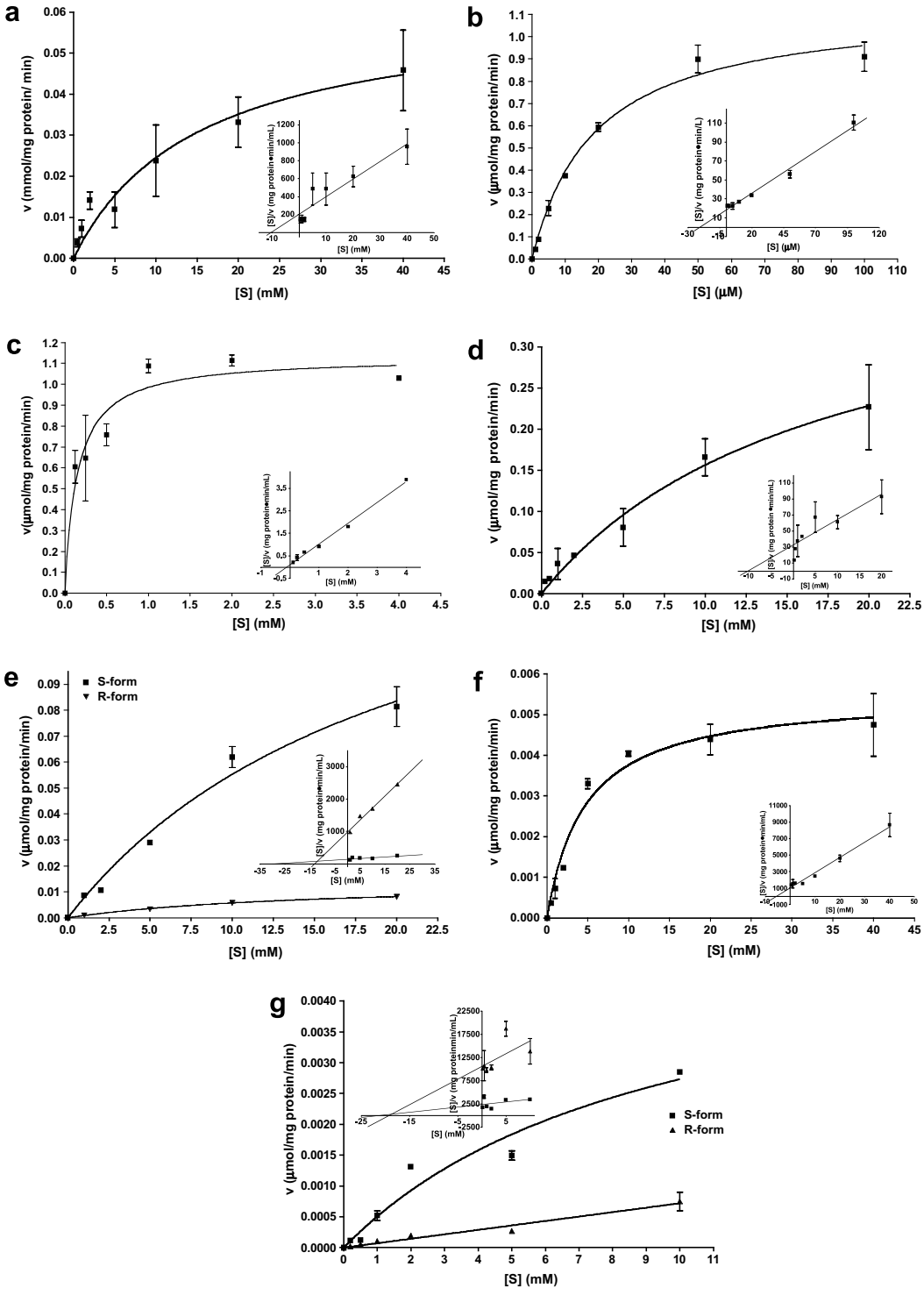

Figure 1. Michaelis–Menten plots and Hanes–Woolf plots of the reduction of *p*-substituted acetophenones by rat liver 3α-HSD. X = H (a); NO_2 (b); CN (c); Br (d); Me (e); OMe (f); NMe_2 (g). Values are presented as means ± SEM of triplicate assays.

Table 1. Variation in the kinetic parameters in the reduction of *p*-substituted acetophenone derivatives by rat liver 3α-HSD

Substrate	Product	Kinetic parameters				Physical parameters		
		K_m[a]	V_{max}[b]	V_{max}/K_m[c]	Ratio[d]	σ_{para}	π	Es
NO_2 (**1b**)	**2b** (*S*)	0.02	1.132	61689.37	N.Dr.[f]	0.78	−0.28	−2.52
	2b (*R*)	N.Dc.[e]	N.Dc.[e]	N.Dr.[f]				
CN (**1c**)	**2c** (*S*)	0.11	1.084	9442.51	N.Dr.[f]	0.66	−0.57	−0.51
	2c (*R*)	N.Dc.[e]	N.Dc.[e]	N.Dr.[f]				
Br (**1d**)	**2d** (*S*)	10.35	0.315	30.56	N.Dr.[f]	0.23	0.86	−1.16
	2d (*R*)	N.Dc.[e]	N.Dc.[e]	N.Dr.[f]				
H (**1a**)	**2a** (*S*)	10.40	0.510	49.00	N.Dr.[f]	0	0	0
	2a (*R*)	N.Dc.[e]	N.Dc.[e]	N.Dr.[f]				
Me (**1e**)	**2e** (*S*)	27.71	0.200	7.21	7.13	−0.17	0.56	−1.24
	2e (*R*)	13.20	0.013	1.01				
OMe (**1f**)	**2f** (*S*)	5.59	0.005	0.97	N.Dr.[f]	−0.27	−0.02	−0.55
	2f (*R*)	N.Dc.[e]	N.Dc.[e]	N.Dr.[f]				
NMe_2 (**1g**)	**2g** (*S*)	21.85	0.009	0.41	4.56	−0.83	0.18	−999
	2g (*R*)	19.22	0.002	0.09				

[a] mM.
[b] μmol (mg protein)$^{-1}$ min^{-1}.
[c] μL (mg protein)$^{-1}$ min^{-1}.
[d] $(V_{max}/K_m)_S/(V_{max}/K_m)_R$.
[e] N.Dc: Not detected.
[f] N.Dr.: Not determined.

cyano (**1c**) or bromo (**1d**) substituent to the benzene ring enhanced the reduction rate, whereas introduction of an electron-releasing group such as an *N*,*N*-dimethylamino (**1g**), methoxyl (**1f**) or methyl (**1e**) substituent to the benzene ring lowered the rate. These results indicate that the reaction rate depends on the electron density of the carbonyl carbon of the acetophenone. Figure 2a shows the Hammett plots for the reduction of substituted acetophenones using rat 3α-HSD, consisting of plots of $\log\{(V_{max}/K_m)X/(V_{max}/K_m)H\}$ versus values $(-0.52\pi + 3.83\sigma_{para} - 0.001Es - 0.30)$ that were calculated by the least-square method. The plots afford a straight line with a slope of $\rho = +1.00$ (correlation coefficient $(r^2) = 0.97$). These plots showed that the reduction of *para*-substituted acetophenones by rat liver 3α-HSD is strongly influenced by the electron density of the carbonyl carbon of the acetophenone but not by the hydrophilicity or size of the substituent.

These data provide some insight into the reaction mechanism for hydride transfer during the enzymatic reaction. The plots of $\log\{(V_{max}/K_m)X(V_{max}/K_m)H\}$ versus σ_{para} also show linear correlations (Fig. 2b). The positive ρ (+3.3) value indicates that a δ^- charge was generated at the phenyl carbon adjacent to the carbonyl group generating in the transitional state (compared to the initial state). Mechanistic studies using Hammett plots of the hydride transfer reactions in chemical[9–14] and enzymatic[15] systems have been reported. Relatively

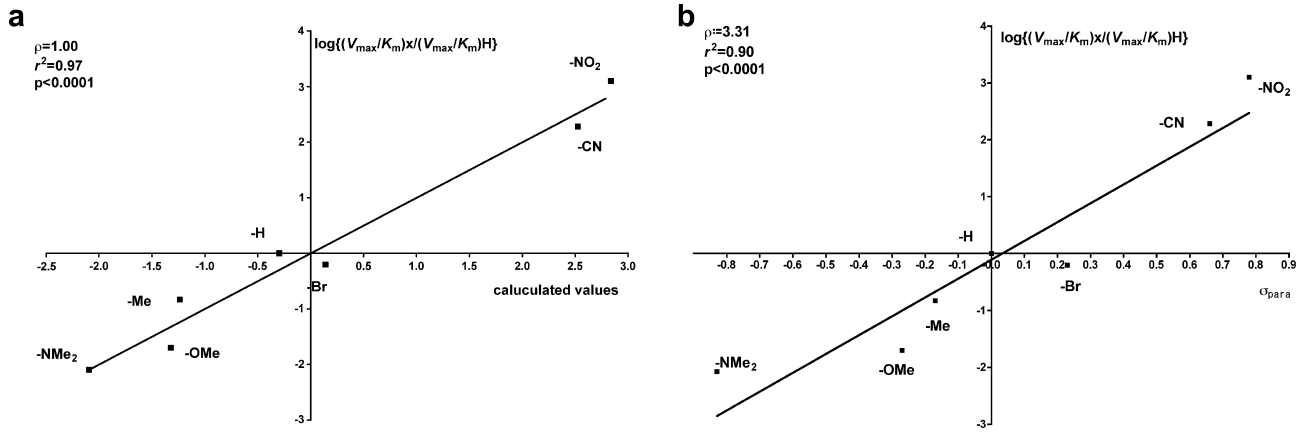

Figure 2. (a) Correlation between $\log\{(V_{max}/K_m)X/(V_{max}/K_m)H\}$ values and calculated values $(-0.52\pi + 3.83\sigma_{para} - 0.001Es - 0.30)$ in the reduction of *p*-substituted acetophenone derivatives by rat liver 3α-HSD. (b) Correlation between $\log\{(V_{max}/K_m)X/(V_{max}/K_m)H\}$ values and σ_{para} in the reduction of *para*-substituted acetophenone derivatives by rat liver 3α-HSD.

low ρ values (0.7–1.2) were observed in the reduction of aryl ketones by crude carbonyl reductases of the human liver.[15] In the chemical reaction systems, low ρ values were reported for the Meerwein–Ponndorf–Verly (MPV) reaction by supercritical 2-propanol[9] (ρ + 0.33) and moderate ρ values were seen in the MPV reaction by metal alkoxide (ρ + 1.3–1.7)[10–12] and in the metal hydride reaction[13,14] (ρ + 1.9–3.1). Our present results indicate that enzymatic reduction shows ρ values that are similar to those with the MPV reaction by supercritical 2-propanol. In the present reaction, the enzyme displays an ordered bi–bi kinetic mechanism in which binding of the nicotineamide cofactor is an obligatory requirement before substrate can bind, and direct hydride transfer occurs from the C4 position of the nicotineamide ring to the acceptor carbonyl of the substrate which is protonated by Y55 that acts as a general acid, and this chemical event would be the rate limiting step.[16] Thus, the strength of the acidity of the Y55 may also contribute to determination of the rate of the carbonyl reduction.

In any case, our findings show that acetophenone derivatives containing an electron-withdrawing group at the *para* position were reduced faster than those with an electron-donating group. This indicates that the reductive metabolism of drugs having aromatic ketones, such as haloperidol, depends on the substituent at the *para* position of the aromatic ring, and an electron-withdrawing group promotes the metabolism.

The abnormally large V_{max}/K_m values of the nitro and cyano derivatives (**1b** and **1c**) can be explained by the relatively small K_m value of the substrate. The K_m value increased according to the increase in the electron-donating property of the substituent, except for the case of the methoxy group. This suggests that the enzyme has an amino acid residue(s) that can interact with the oxygen moiety at the *para* position of the substrate. In that case, nitro (**1b**) and methoxy substrates (**1f**) will show smaller K_m values compared to the other substrates.

The influence of the electronic effects on the enantioselectivity can be surmised by comparison of the V_{max}/K_m value of the *S*-enantiomer with that of *R*. The enantioselectivity of the reduction is subject to a remote electronic effect on the substrate ketones. As seen in the 'ratios' presented in Table 1, *R*-enantiomers were not recognized at all on HPLC in the reduction of electron-withdrawing moiety substituted acetophenones. However, reduction of electron-donating methyl-(**1e**) and *N*,*N*-dimethyl-(**1g**) substituted acetophenones gave (*R*)-enantiomers at a relatively higher 'ratio'. Thus, ketones with an electron-withdrawing group in the *para*-position of the aromatic ring might better afford enantioselectively reduced alcohols compared to electron-donating groups.

3. Conclusions

This study demonstrated an electron-withdrawing effect on the reduction rate in enzymatic conversion of carbonyl compounds to the corresponding alcohols. With this in mind, new drugs can be designed that exploit this reduction pathway by introducing an electron-withdrawing group adjacent to the reduction site when a reduction reaction is desired or by adding an electron-donating group when minimization of the reduction pathway is desired.

4. Materials and methods

4.1. Chemicals

Para-nitro- and methoxy-acetophenones and acetophenone were purchased from Wako Pure Chemical Industries, Ltd. (Osaka, Japan). *Para*-cyano- and *N*,*N*-dimethylacetophenones were purchased from Tokyo Kasei Kogyo Co., Ltd. (Tokyo, Japan). *Para*-bromo- and methyl- acetophenones were purchased from Nakarai Tesque, Inc. (Kyoto, Japan). $NADP^+$ and glucose 6-phosphate (G-6-P) were procured from Nacalai Tesque, Inc. Glucose-6-phosphate dehydrogenase (G-6-P-D) was purchased from Sigma Chemical Co. (St. Louis, MO, USA). All other chemicals and solvents were of the highest commercially available grade.

4.2. Instruments

All chemical reactions were conducted in oven-dried glassware. Silica gel 60 (70–230 mesh, ASTM, Merck) was used for column chromatography. Precoated Kieselgel 60F-254 plates (0.25 mm, Merck) were used for TLC analysis, and the spots were detected by the absorption of UV light at 254 nm by spraying anisaldehyde–sulfuric acid reagent followed by heat treatment. Optical rotations were measured on JASCO DIP-360 polarimeters. ^{1}H- and ^{13}C-NMR spectra were recorded on JEOL JNM EX270 (270 MHz), JEOL JNM 400 (400 MHz) and JEOL JNM 600 (600 MHz) spectrometers. Mass spectra were recorded on JEOL JMS DX-303/JMA-DA 5000 spectrometers. The quantitative analyses, enantiomeric excess (ee) and absolute configurations of the alcohols were determined by HPLC using a Waters 510 HPLC Pump (Waters, Milford, MA, USA) that was equipped with a chiral column. The eluate was monitored at 254 nm using a Waters 486 Tunable Absorbance Detector (Waters, Milford, MA, USA). Chromatographs were recorded using a Chromatocorder 21 (S.I.C., Tokyo, Japan).

4.3. Synthesis of authentic samples of reduced aryl ketones

Alcohols were synthesized by reducing the aryl ketones with $NaBH_4$ (0.25 mol equivalent) followed by purification by silica gel column chromatography. The produced alcohols were subjected to lipase catalyzed transesterification to afford chiral alcohols, and their optical rotatory powers were referenced to the reported data.

4.4. Enzyme purification

Rat liver 3α-HSD was isolated, and the reductase activity was assayed according to our previously reported method.[8]

4.5. Protein quantification

The protein concentration was determined by the method of Bradford et al.[17] with bovine serum albumin as the standard.

4.6. Reduction of aryl ketones by rat liver 3α-HSD (general procedure)

A typical incubation mixture consisted of 10 mM sodium potassium phosphate buffer (PBS, pH 7.4), an NADPH-generating system (1.3 mM NADP, 10 mM G-6-P, 0.04 U/mL of G-6-P-D and 5 mM $MgCl_2$) and rat liver 3α-HSD in a total volume of 400 μL. The protein content and reaction time were predetermined based on linearity between the rat liver 3α-HSD concentration and the reaction time, and the metabolite-formation rate (Table 2). Each experiment was performed in triplicate. The mixture was preincubated for 3 min at 37 °C in air. The reaction was initiated by addition of 100 μL of a solution of the substrate in PBS. After incubation at 37 °C for the indicated time (Table 2), 500 μL of a solution of the internal standard (Table 2) in AcOEt was added to stop the reaction. The mixture was extracted with AcOEt and centrifuged at 6750*g* for 5 min. The organic layer was transferred to another tube and concentrated in vacuo. The residue was dissolved in 50 μL of the solvent used as the mobile phase in the HPLC analyses, and 10 μL of the solution was subjected to HPLC analysis. The metabolite was quantified by comparing the HPLC peak area that was monitored at 254 nm to that of the internal standard.

4.7. HPLC conditions

4.7.1. 1-Phenylethanol (2a). A Chiralcel OD-H column (4.6 × 250 mm, 5 μm; Daicel Chemical Industries, Ltd.) was used and eluted with *n*-hexane-2-propanol (49:1 v/v) at 1.0 mL/min. t_R = 16.9 min for (*R*)-1-phenylethanol, and t_R = 21.1 min for (*S*)-1-phenylethanol.

4.7.2. α-Methyl-*p*-nitrobenzyl alcohol (2b). A Chiralpak AD-H column (4.6 × 250 mm, 5 μm; Daicel Chemical Industries, Ltd.) was used and eluted with *n*-hexane-2-propanol (97:3 v/v) at 0.5 mL/min. t_R = 35.0 min for (*R*)-α-methyl-*p*-nitrobenzyl alcohol, and t_R = 36.2 min for (*S*)-α-methyl-*p*-nitrobenzyl alcohol.

4.7.3. α-Methyl-*p*-nitrilebenzyl alcohol (2c). A Chiralcel OJ-H column (4.6 × 250 mm, 5 μm; Daicel Chemical Industries, Ltd.) was used and eluted with *n*-hexane-2-propanol (9:1 v/v) at 1.0 mL/min. t_R = 16.92 min for (*R*)-α-methyl-*p*-nitrilebenzyl alcohol, and t_R = 14.33 min for (*S*)-α-methyl-*p*-nitrilebenzyl alcohol.

4.7.4. α-Methyl-*p*-bromobenzyl alcohol (2d). A Chiralcel OJ-H column (4.6 × 250 mm, 5 μm; Daicel Chemical Industries, Ltd.) was used and eluted with *n*-hexane-2-propanol (95:5 v/v) at 0.5 mL/min. t_R = 15.85 min for (*R*)-α-methyl-*p*-bromobenzyl alcohol, and t_R = 14.76 min for (*S*)-α-methyl-*p*-bromobenzyl alcohol.

4.7.5. α-Methyl-*p*-methylbenzyl alcohol (2e). A Chiralcel OJ-H column (4.6 × 250 mm, 5 μm; Daicel Chemical Industries, Ltd.) was used and eluted with *n*-hexane-2-propanol (95:5 v/v) at 0.5 mL/min. t_R = 16.11 min for (*R*)-α-methyl-*p*-methylbenzyl alcohol, and t_R = 14.23 min for (*S*)-α-methyl-*p*-methylbenzyl alcohol.

4.7.6. *p*-Methoxy-α-methylbenzyl alcohol (2f). A Chiralcel OD-H column (4.6 × 250 mm, 5 μm; Daicel Chemical Industries, Ltd.) was used and eluted with *n*-hexane-2-propanol (98:2 v/v) at 1.0 mL/min. t_R = 28.28 min for (*R*)-*p*-methoxy-α-methylbenzyl alcohol, and t_R = 22.46 min for (*S*)-*p*-methoxy-α-methylbenzyl alcohol.

4.7.7. *p*-Methoxy-α-methylbenzyl alcohol (2g). A Chiralpak AS-H column (4.6 × 250 mm, 5 μm; Daicel Chemical Industries, Ltd.) was used and eluted with *n*-hexane-2-propanol (9:1 v/v) at 1.0 mL/min. t_R = 9.29 min for (*R*)-*p*-methoxy-α-methylbenzyl alcohol, and t_R = 13.78 min for (*S*)-*p*-methoxy-α-methylbenzyl alcohol.

Table 2. The reaction conditions for substrates (–NO_2, –CN, –Br, –H, –Me, –OMe, –NMe_2)

	Time (min)	Protein (μg protein/mL)	Internal standard
–NO_2	5	12	3-Acetylpyrrole
–CN	10	7.5	2,6-Diacetylpyridine
–Br	12	20	2,6-Diacetylpyridine
–H	30	50	2,6-Diacetylpyridine
–Me	30	30	2,6-Diacetylpyridine
–OMe	60	75	2-Acetylpyrrole
–NMe_2	40	50	3-Acetylpyrrole

4.8. Analysis of kinetic data

The maximum velocity (V_{max}) and Michaelis–Menten constant (K_m) were calculated from Hanes–Woolf plots using the untransformed kinetic data and a personal computer.

References and notes

1. Penning, T. M.; Mukharji, I.; Barrows, S.; Talalay, P. *Biochem. J.* **1984**, *222*, 601.
2. Takikawa, H.; Stolz, A.; Kuroki, S.; Kaplowitz, N. *Biochim. Biophys. Acta.* **1990**, *1043*, 153.
3. Smithgall, T. E.; Harvey, R. G.; Penning, T. M. *J. Biol. Chem* **1986**, *261*, 6184.
4. Penning, T. M.; Sharp, R. B. *Biochem. Biophys. Res. Commun.* **1987**, *148*, 646.
5. Ikeda, M.; Hattori, H.; Ohmori, S. *Biochem. Pharmacol.* **1984**, *33*, 3957.
6. Yamano, S.; Nakamoto, N.; Toki, S. *Xenobiotica* **1999**, *29*, 917.

7. Ikawa, H.; Fernandez-Checa, J. C.; Kuhlenkamp, J.; Stolz, A.; Ookhtens, M.; Kaplowitz, N. *Biochim. Biophys. Acta* **1991**, *1084*, 247.
8. Uwai, K.; Konno, N.; Kitamura, S.; Ohta, S.; Takeshita, M. *Chirality* **2005**, *17*, 494.
9. Kamitanaka, T.; Matsuda, T.; Harada, T. *Tetrahedron* **2007**, *63*, 1429.
10. Pickart, D. E.; Hancock, C. K. *J. Am. Chem. Soc.* **1955**, *77*, 4642.
11. Burnett, R. D.; Kirk, D. N. *J. Chem. Soc., Perkin Trans. II* **1976**, 1523.
12. Wigfield, D. C.; Gowland, F. W. *Tetrahedron Lett.* **1979**, *20*, 2209.
13. Wiegers, K. E.; Smith, S. G. *J. Am. Chem. Soc.* **1977**, *99*, 1480.
14. Bowden, K.; Hardy, M. *Tetrahedron* **1966**, *22*, 1169.
15. Wong, J. M. Y.; Mahon, W. A.; Kalow, W.; Inaba, T. *Drug Metab. Disp.* **1992**, *20*, 465.
16. Heredia, V. V.; Penning, T. M. *Biochemistry* **2004**, *43*, 12028.
17. Bradford, C. M. *Anal. Biochem.* **1976**, *72*, 248.